AUTOMATED QUANTITATION OF NON-STEADY FLOW AND LUMEN AREA BASED ON TEMPORAL CORRELATION

Sang H. Lee, Noam Alperin

Department of Radiology, University of Illinois at Chicago, Chicago, Illinois USA

Abstract – **A robust method for automated quantitation of nonsteady flow and lumen area is presented. The method utilizes temporal information to differentiate between pixels within the lumen and a background region. Cross correlation (CC) is applied to identify the pixels with temporal information similar to a reference obtained from a pixel within the lumen region. The new method incorporates a computation of an optimal threshold; therefore, it provides an unbiased observer-independent quantitation. We have conducted in vitro and in vivo experiments to evaluate the reproducibility and accuracy of the method.**

Keywords – **nonsteady flow, volumetric flow quantitation, automated lumen segmentation.**

I. INTRODUCTION

Quantitation of blood flow provides important information in evaluation of cardiovascular diseases (1). Measurement of hemodynamic changes in renal artery has been used to study the clinical implications of renal artery stenosis (2). Quantitation of cerebrospinal fluid (CSF) has become important in diagnosis of CSF related disorders such as pseudotumor cerebri (chronically elevated intracranial pressure (ICP)), and Chiari malformation (herniation of hindbrain into the spinal canal) (3,4). Recently, noninvasive method to measure intracranial pressure from measurements of blood and CSF flow has been developed. This method utilizes quantitation of arterial, venous and CSF flow to derive ICP and compliance (5).

A motion sensitive MRI technique, dynamic phase contrast, is becoming the gold standard method of quantifying volumetric flow rates (6). In this technique, magnetic field gradients are applied to generate phase shifts for moving spins. The resulted phase maps are proportional to the spins' velocities (6). Dynamic implementation of this technique enables imaging of non-steady flow during the cardiac cycle. The total flow through the lumen can be calculated by integrating the pixel intensities within the lumen. In order for this technique to be reliably applied to clinical cases, accurate and reproducible volumetric flow rate measurements are essential. Manual identification of lumen boundary is still the most commonly used method. However, due to its operator's skill dependency, manual segmentation can be inconsistent and inaccurate.

Several automated methods have been proposed. Burkart et. al. (7) segmented lumen by thresholding the intensity of a single magnitude image. Hu et. al. (8) used a region growing technique with intensity threshold to segment the entire vascular structure in 3 dimensional MRI images of blood vessels. Kozerke et. al. (9) used an active contour technique, which utilizes a deformable contour balancing two different energy fields, to find the most outer edge of the vessel lumen. Oyre et. al. (10) segmented lumen of vessel conducting laminar flow by fitting the velocity map within the lumen to three-dimensional paraboloid. Baledent et. al. (11) proposed a method to segment lumens conducting Oscillatory flow such as CSF flow. A Fourier Transform of the temporal dynamics of each pixel is calculated and pixels that the first harmonic is larger than DC value are selected.

While most methods utilize spatial information from a single image, the new method utilizes multiple images. Differences in <u>*temporal*</u> information between pixels located in the lumen and in the surrounding tissue are utilized as segmentation criteria. The dynamic information of the lumen is sampled and used as a reference to search for a similar temporal behavior by comparing the velocity waveforms of the pixels around this region. CC is applied to quantify the degree of similarity between a reference waveform and the waveforms obtained from the surrounding pixels. The performance of this method was evaluated in vitro and in vivo experiments.

II. METHODOLOGY

The automated procedure includes four steps:

1) selecting a reference velocity waveform
2) generating CC map
3) computing optimal CC threshold
4) tracking the edge of the segmented region

Selecting reference velocity waveform

An example of a phase contrast MR velocity image of the arteries and veins in the neck is shown in Figure

Report Documentation Page

Report Date	Report Type	Dates Covered (from... to)
25OCT2001	N/A	-

Title and Subtitle	Contract Number
Automated Quantitation of Non-Steady Flow and Lumen Area BAsed on Temporal Correlation	
	Grant Number
	Program Element Number

Author(s)	Project Number
	Task Number
	Work Unit Number

Performing Organization Name(s) and Address(es)	Performing Organization Report Number
Department of Radiology, University of Illinois at Chicago, Chicago, Illinois	

Sponsoring/Monitoring Agency Name(s) and Address(es)	Sponsor/Monitor's Acronym(s)
US Army Research, Development & Standardization Group (UK) PSC 802 Box 15 FPO AE 09499-1500	
	Sponsor/Monitor's Report Number(s)

Distribution/Availability Statement
Approved for public release, distribution unlimited

Supplementary Notes
Papers from the 23rd Annual International Conference of the IEEE Engineering in Medicine and Biology Society, 25-28 OCT 201, held in Istanbul, Turkey. See also ADM001351 for entire conference on cd-rom., The original document contains color images.

Abstract

Subject Terms

Report Classification	Classification of this page
unclassified	unclassified

Classification of Abstract	Limitation of Abstract
unclassified	UU

Number of Pages
4

1a. The location of a pixel that is used as a "reference waveform" is marked by the x. Figure 1b shows the velocity waveform at that location.

Generating CC map

The CC coefficient, as defined in equation 1, is used to quantify similarity between the reference waveform and waveforms obtained from other pixels in the image.

$$P_{XY} = \frac{\sum_{k=0}^{N} (R_k - \overline{R})(XY_k - \overline{XY})}{\sqrt{\sum_{k=1}^{N} (R_k - \overline{R})^2 \sum_{k=1}^{N} (XY_k - \overline{XY})^2}} \quad (1)$$

P_{xy} is the CC value at pixel location XY, R is the reference waveform, k is the time index of the time-series images, and N is the total number of images in the time series. A grayscale map proportional to the CC coefficient calculated for each pixel location is generated and is shown in figure 1C where higher pixel intensity represents higher CC value.

Computing optimal CC threshold

A histogram of number of pixels with CC value above the threshold for different threshold values is generated. An example of a typical histogram is shown in figure 1D. Such a histogram contains three regions:

1) Region A – Rapid increase in the number of pixels as threshold decreases. The region corresponds to pixels within the lumen.
2) Region B – Relatively small increase. This region corresponds to pixels that are located near the edge of the lumen and some in background region.
3) Region C – A rapid increase. Identified pixels are mainly located outside the lumen of interest.

The optimal threshold CC value is selected at the point of transition from region B to region C.
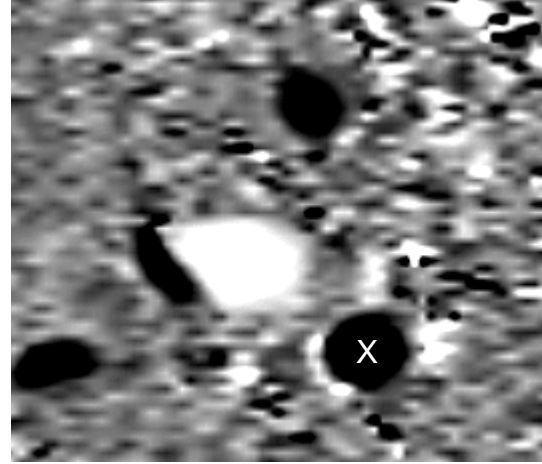
Tracking the edge of the segmented region

The boundary of the segmented pixels with CC value above threshold is identified by tracking the nearest neighbor pixel that is:
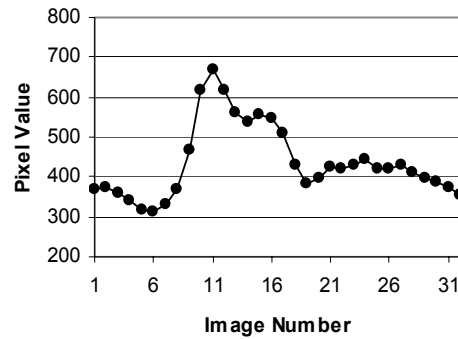1) above the threshold and
2) neighboring with pixels that are below the threshold.
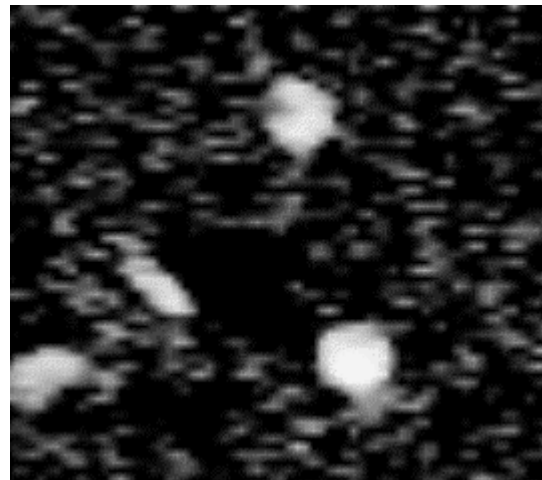An example of a lumen with edge traction applied is shown in figure 1E.
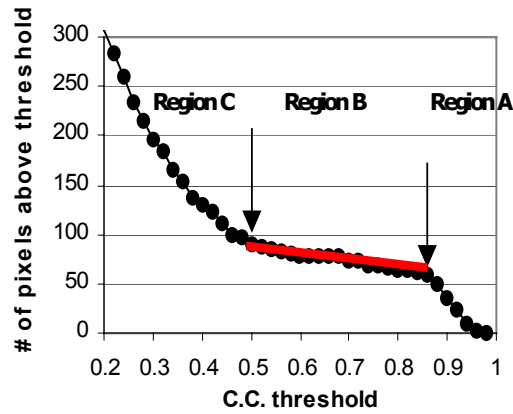
FIGURE 1

A) Phase contrast image with location of the reference waveform.
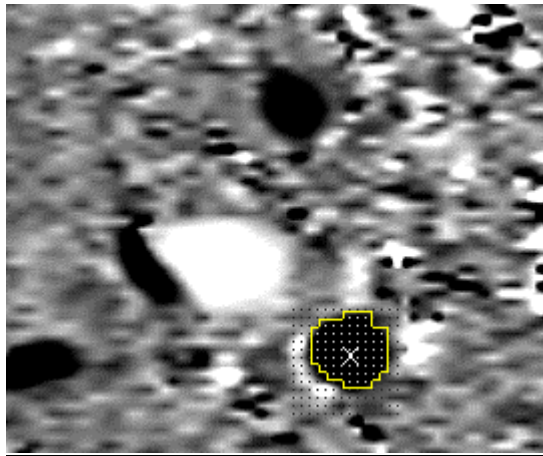

B) Reference waveform during one cardiac cycle.

C) Grayscale CC map.

D) CC threshold vs. # of pixels above threshold.

E) Lumen with edge traction applied.

EXPERIMENTS

A phantom experiment was performed using a 1.5 T MRI scanner (GE medical systems, Milwaukee). Three different flow setups were evaluated. For flow setup 1, three repeated scans were performed with the following MRI parameters: Velocity encoding (VENC) = 75cm/s, FOV = 20*20cm, TR/TE = 18/5msec. Flow setup 2 and 3 were repeated 8 and 5 times, respectively, and scanning was performed on a 3T scanner with the MRI parameters: VENC = 75cm/s, FOV = 16*16cm, and TR/TE = 18/6.3msec. Averages and % standard deviations of each lumen's flow rate and diameter were calculated.

To evaluate the performance of the method on patients' data, 15 data sets, each includes 2 internal carotid arteries, 2 vertebral arteries, 2 jugular veins, and CSF flow at the level of C2, were analyzed by 5 observers using both manual and automated segmentation. Reproducibility was compared between the two segmentation techniques.

III. RESULTS

Means and % standard deviations (%SD) of area, flow rate, and diameter for each in vitro lumen are listed on Table I. Lumens 1, 2, and 3 have same lumen area and lumen 4 has a smaller area. The %SD for each in vivo measurement done both manual and automated techniques is summarized in Table II.

TABLE I
IN VITRO: Accuracy and Reproducibility

Flow Setup	Lumen		Area mm^2	Flow ml/min	Diameter mm
1*	1	mean	50.6	339.1	8.03
		% SD	1.48	1.10	0.84
	2	mean	49.6	343.0	7.95
		% SD	3.02	1.95	1.51
	3	mean	49.6	359.7	7.95
		% SD	1.51	3.10	0.75
2*	1	mean	52.1	257.1	8.19
		% SD	2.24	1.41	1.02
	2	mean	51.9	256.2	8.18
		% SD	1.50	3.71	0.91
	3	mean	49.4	271.1	7.96
		% SD	1.41	1.87	0.48
3	1	mean	47.0	105.4	7.77
		% SD	3.01	2.92	1.37
	2	Mean	48.2	101.2	7.87
		% SD	2.75	6.60	1.46
	3	mean	48.4	124.6	7.88
		% SD	1.65	2.41	0.87
	4	mean	27.4	147.8	5.96
		% SD	3.72	3.74	1.73

Table I.   Independent measurements of true flow rate were not available. True diameter of lumen 1,2,3 is 8 mm. True diameter of lumen 4 is 6 mm. (%SD = SD/mean*100) * Due to alias, lumen 4 was not measured for setup 1and 2.

TABLE II
IN VIVO: Reproducibility

Lumen	# of pixel ml/min		Manual % SD	Automated % SD
Carotid Artery	Area	R	9.9	2.0
		L	9.6	2.4
	Mean flow		30.6	5.6
Jugular Vein	Area	R	18.5	4.0
		L	7.8	4.2
	Mean flow		56.7	12.3
Vertebral Artery	Area	R	9.2	1.8
		L	8.3	2.0
	Mean flow		23.4	5.7
CSF	Area		30.3	7.4
	Osc. Flow		1.3	0.6

Table II.   %SD is compared between the two techniques.

The average area and diameter for all in vitro flow setup (lumen 1, 2, and 3) are 49.63mm^2 and 7.98mm with average %SD of 2.05% and 1.01%, respectively. Actual dimensions are 50.27mm^2 and 8.00mm, respectively. Lumen 4 has average area and diameter of 27.4mm^2 and 5.96mm with average %SD of 3.72% and 1.73% where actual area and diameter are 28.2mm^2 and 6.00mm, respectively. Flow rate setup is only available for flow setup 1. The average flow rate and %SD are 354.4ml/min and 2.25%, respectively, where actual setup is 366ml/min.

Table II summarizes the user-variability measured with manual and automated method. Improvement factors (Manual %SD / Automated %SD) which averaged for all vessels' areas and flows are 4.11 and 4.73, respectively. (CSF oscillatory flow was not included for this calculation.)

IV. DISCUSSION

Validation of the accuracy of the automated method was performed only on a phantom study since there is no other method that can provide the true lumen size measurement in vivo. The errors obtained with the automated method for different lumen sizes ranged from 0.37% to 2.88%. This compared favorably with larger errors ranging from 6.50% to 10.88% that were found by other sites using the same phantom in a multi-center trial.

The reproducibility of the automated method was evaluated using MRI data from subjects. The reproducibility of lumen size measurements of in vivo study improved significantly. On the average, the automated method produced results that were more reproducible by a factor of 4.11 for area and 4.73 for flow rate. Burkart (7) has compared user-variability between magnitude threshold method and manual method by measuring the flow of the portal vein. Their result shows that user-variability of magnitude threshold method was reduced by a factor of only 2.69 over manual method.

Visual determination of the lumen border is influenced by the noise levels and window settings of the viewed image. The temporally correlated method utilizes information from multiple images and therefore information with higher SNR is available for determining the lumen. The location of a pixel that is used as a "reference waveform" does not affect the results significantly.

In summary, the automated segmentation based on temporal correlation provides accurate and reproducible quantitation of the lumen size and flow rate for non-steady flow.

REFERENCES

[1] Alperin N, Hoffmann KR, Doi K, Chua KG. Automated analysis of coronary lesions from cineangiograms using vessel tracking and iterative deconvolution techniques. Computers in Cardiology, IEEE, 153-156 (1990).

[2] Missouris CG, Buckenham T, Cappuccio FP, MacGregor GA: Renal Artery Stenosis: A Common and Important Problem in Patients with Peripheral Vascular Disease, Am J. Med., Jan 96(1):10-4 (1994).

[3] Gjerris F, Soelberg P, *et.al.*: Intracranial Pressure, conductance to CSF Outflow, and Cerebral Blood Flow in Patients with Benign Intracranial Hypertension (PTC), Ann Neurol 17:158-162 (1985).

[4] Pujol J, Roig C, *et. al.*: Motion of the Cerebellar Tonsils in Chiari Type I Malformation Studied by Cine Phase-Contrast MRI, Neurology 45:1746-1753 (1995).

[5] Alperin N, Lee SH, *et. al.*: MR-ICP: A Method to Measure Intracranial Elastance and Pressure Noninvasively by Means of MR Imaging, Radiology 217(P):877-885 (2000).

[6] Pelc N, Herfkens R, Shimakawa A, Enzmann D: Phase Contrast Cine Magnetic Resonance Imaging, Magn. Reson. Q. 7,229-254 (1991).

[7] Burkart D, Felmlee F, *et. al.*: Cine Phase-Contrast MR Flow Measurement: Improved Precision using an Automated Method of Vessel Detection, Journal of Computer Assisted Tomography 18(3):469-475, May/June, (1994).

[8] Hu X, Alperin N, *et. al.*: Visualization of MR Angiographic Data with Segmentation and Volume-rendering Techniques, Journal of Mag. Res. Imaging, Vol, No.5, pp.539-546, Sep/Oct (1991).

[9] Kozerke S, Botnar R, *et. al.*: Automated Vessel Segmentation Using Active Contours in Cine Phase Contrast Flow Measurements, JMRI 10:41-51 (1999).

[10] Oyre S, Ringgaard S, et. al.: Quantitation of Circumferential Subpixel Vessel Wall Position and Wall Shear stress by Multiple Sectored Three Dimensional Paraboloid Modeling of Velocity Encoded Cine MR, MRM 40:645-655 (1998).

[11] Baledent O, Didon-Poncelet, Hemy-Feugeas, Idy-peretti: Study of Cerebrospinal Fluid Dynamics from Phase Contrast Cine Magnetic Resonance Imaging, Proceedings of International Society for Mag. Res. In Medicine, 7th Scientific Meeting, Philadelphia, Pennsylvania, p2176 (1999).

[12] Summers P, Holdsworht D.W., Nikolov H, Rutt B: Proc. Intl. Soc. Mag. Reson. In Med. Vol. 8:458 (2000).

[13] Lee S, Alperin N: Proc. Intl. Soc. Mag. Reson. In Med. Vol. 2:1540, (2000).